Appl. Phys. B 41, 109–117 (1986)

Applied Physics B Photophysics and Laser Chemistry

CO_2-Laser-Induced Breakdown in Mono- and Diatomic Gases*

J. Blazejowski** and F. W. Lampe

Davey Laboratory, Department of Chemistry, The Pennsylvania State University, University Park, PA 16802, USA

Received 17 December 1985/Accepted 21 May 1986

Abstract. Several monoatomic and homonuclear diatomic gases absorb energy from a focused CO_2-laser photon field. It has been established that the pressure threshold for the energy absorption correlates qualitatively with the known ionization potentials of those gases. The simplified phenomenological theory of the CO_2-laser-induced dielectric breakdown of gases is invoked to explain this phenomenon. In the H_2–D_2 system, the formation of HD is observed under these conditions. The examination of the reaction yields for HD formation demonstrates that the system studied does not reach equilibrium under our experimental conditions. Considerations regarding kinetics of primary processes reveal that ionic species, created originally via an inverse bremsstrahlung mechanism, are converted into atomic transients in fast ionic association processes. The latter species initiate chain reactions with surrounding molecules of substrates leading to the formation of HD. Simple kinetic analysis based on a non-steady-state assumption permitted the derivation of an expression for the yield of HD formation. This equation was fitted to the experimental data assuming that the temperature of the reaction rises with an increase of the amount of D_2 in the mixture. Some other aspects regarding the behavior of this system in a focused CO_2 laser beam are also discussed.

PACS: 82.50, 82.30, 42.60

Mono- and homonuclear diatomic gases are transparent to infrared radiation, in accord with single-photon selection rules. It has also been confirmed experimentally that such substances are transparent to parallel CO_2-laser beams of moderate fluences. In the early 70's several authors reported, however, that these gases absorb energy from a focused CO_2-laser photon field [1–6]. Despite numerous experimental [1–17] and theoretical [9, 14, 15, 17–26] works devoted to this problem, some aspects still remain unexplained. A number of the features observed have been elucidated in the past on the basis of various phenomenological theories of the laser-induced dielectric breakdown of gases. One of those theories, outlined by Hacker et al. [8, 11, 14] has been invoked in this work to elucidate the correlation between the pressure threshold for the energy absorption and the ionization potential of an absorbing gas. Isotopic exchange processes in the H_2–D_2 system have been very widely examined in the past [27–36]. In this work we have investigated some aspects of the chemistry of H_2–D_2 system in a focused CO_2-laser field. This paper is a report of our findings.

1. Experimental

The source of infrared radiation was a pulsed CO_2 TEA laser (Lumonics, Model 103–2) tuned to the P(20) line (944.2 cm^{-1}). The laser beam was stopped down by a metal aperture to an area of 2 cm^2 and then focused into the center of the cells by a BaF_2 lens (focal length: 10 cm) placed just at the entrance windows of the cell. The laser was operated at 0.5 Hz and three

---

* U.S. Department of Energy Document No. DE-AS02-76ER03416-37

** Permanent address: Institute of Chemistry, University of Gdansk, PL-80-952 Gdansk, Poland different compositions of lasing gas, which allowed measurements to be performed at different beam temporal profiles [37]. The amounts of energy deposited (E_{abs}) and/or incident pulse energy (E_0) were measured by a Gen-Tec (Model ED-500) joulemeter, placed beyond the exit windows of the cells. The breakdown-threshold experiments were conducted in a stainless steel cell (optical length: 15.5 cm) equipped with one pair of NaCl windows, transparent to the ir radiation, and another pair of standard glass windows enabling visual observation of the luminescence at right angles to the beam axis. The cell was evacuated and filled with gas sample at pressures well above the appropriate threshold value, so that initially the gas would break down on every laser pulse. The pressure of the gas was then decreased in small steps until threshold was crossed and breakdown ceased. In another series of experiments we started from irradiation of an empty cell, gradually increasing the gas pressure until breakdown occurred. Higher pressure threshold values were always found in the latter case. We have taken the mean from both these series of experiments to be the true pressure threshold value for gas breakdown.

In the pressure-threshold measurements, the laser was operated at two different compositions of lasing gas: He : CO_2 : N_2 of 10.0 : 5.0 : 0.0 ("short pulse") and 10.0 : 3.0 : 0.6 ("long pulse") and at constant incident pulse energy equal to 0.85 J/pulse. To keep the incident pulse energy constant the laser beam, in the case of "long pulse", was attenuated by passing it through a cell filled with the appropriate pressure of PH_3 [37].

The irradiations of H_2–D_2 mixtures were performed in a 152 cm^3 (optical length: 15.5 cm) cylindrical stainless steel cell fitted with NaCl windows and coupled via a pinhole leak to a Bendix Model 14–101 time-of-flight mass spectrometer [37]. In these experiments the laser was operated at a constant composition of a lasing gas, namely He : CO_2 : N_2 = 6.0 : 2.0 : 0.7, which assured a high-energy output per pulse (1.60 ± 0.05 J). The changes in concentrations of H_2, D_2, and HD were followed by measurements of the intensities of the ion currents at $m/z = 2$, 4, and 3, respectively. The extent of reaction is reported in terms of reaction yields, $Y(\pm i)$, defined as in (1), i.e.

$$Y(\pm i) = \frac{\text{number of moles of } i \text{ formed } (+) \text{ or decomposed } (-)}{\text{number of pulses}}. \quad (1)$$

As measured values of $Y(-H_2)$, $Y(-D_2)$, and $Y(HD)$ for a given reactant mixture differed somewhat, one from another, we assumed the mean to be a true reaction yield value of HD formation.

He(99.995%), Ne(99.995%), Ar(99.998%), Kr(99.995%), H_2(99.95%), N_2(99.99%), PH_3(99.999%) all from Matheson, and D_2(99.5%, Linde), were used as received. H_2–D_2 mixtures were prepared using a Saunders-Taylor apparatus [38].

2. Results and Discussion

2.1. Correlation Between the Pressure Threshold for Energy Absorption and the Ionization Potential of a Gas Sample

Simple monoatomic and homonuclear diatomic gases can absorb energy from a focused CO_2-laser beam and this process occurs only at high density of electromagnetic radiation. The most characteristic feature of the process is that it exhibits a threshold nature in which the absorption cross section increases sharply when values of certain parameters characterizing the laser photon field and irradiated system attain appropriate threshold values. Furthermore, the energy absorption process is always accompanied by breakdown of the gas sample and strong emission of visible radiation. Similar phenomena have been observed during irradiation of numerous triatomic [39], tetraatomic [37, 40, 41], and even more complex [42–45] molecules, that do not undergo decomposition in a parallel CO_2-laser beam. Ronn [46] states that the pressure threshold for the dielectric breakdown of gases can be related to their polarizabilities. We have noticed that the values of pressure threshold for the breakdown of gases can be also correlated with their ionization potentials (Fig. 1). To explain this dependency we invoked the phenomenological model of the laser-induced dielectric breakdown of gases outlined by Hacker et al. [8, 11, 14]. The authors assume that, under the influence of an intense CO_2-laser field, free electrons (or ions) present originally in the focal volume can be accelerated, owing to the incoherent absorption of energy from the electromagnetic field of radiation (inverse bremsstrahlung absorption). Energized electrons are capable of ionizing neutral molecules in collisions and the newly formed electrons, in turn, absorb energy by an inverse bremsstrahlung mechanism. Multiplication of these processes can provide a large number of electrons for the breakdown avalanche. The threshold conditions are attained if the electron gain rate becomes equal or higher than the electron loss rate. Further, Hacker et al. assumed that the latter effect results from elastic electron-molecule collisions and diffusion of electrons beyond the focal zone. The equation relating the pulse energy threshold (E_{th}) and pressure of absorbing gas

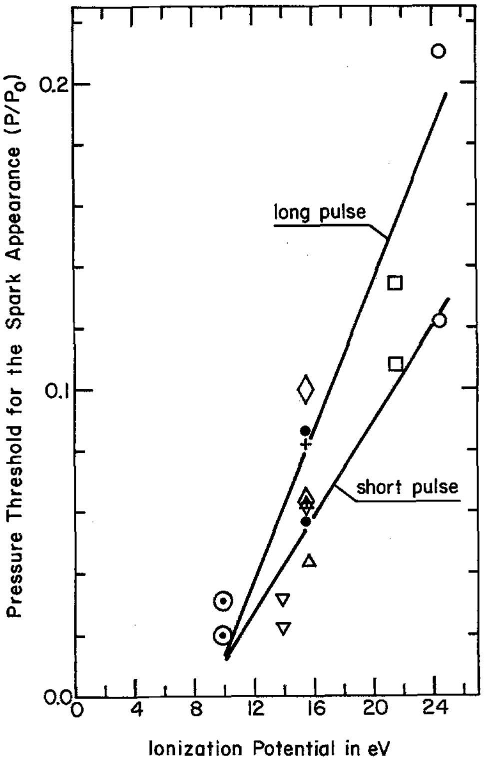

Fig. 1. Pressure threshold of the luminescence appearance for He (○), Ne (□), Ar (△), Kr (▽), H_2 (◇), D_2 (●), N_2 (+), and PH_3 (⊙) versus ionization potential of the absorbing gas sample (P_0 is the atmospheric pressure)

(P) is given by (2)

$$E_{th}=\frac{\varepsilon_0 cm\omega^2 SU_i}{e^2}\left[\frac{2\langle\varepsilon\rangle\tau}{3m\Delta^2\beta^2}\frac{1}{P^2}+\left(\ln\frac{n_b}{n_0}\right)\frac{1}{\beta}\frac{1}{P}+\frac{2m\langle\varepsilon\rangle\tau}{MU_i}\right], \qquad (2)$$

where ε_0 is the permittivity of free space, c is velocity of the light, m and M are the electron and neutral-molecule masses, respectively, ω denotes the laser frequency, S is the laser beam cross-section, U_i represents the ionization potential of gas molecules, e is the electronic charge, $\langle\varepsilon\rangle$ is an average electron energy, Δ represents a diffusion length, τ denotes the pulse duration, β is a constant relating the electron-molecule collision frequency and pressure, and n_b and n_0 denote the critical electron density and the initial electron density, respectively. At constant pulse energy the pressure threshold for breakdown of gases can be expressed by (3), viz.

$$P_{th}=\frac{b}{2a}+\sqrt{\left(\frac{b}{2a}\right)^2+\frac{c}{a}}, \qquad (3)$$

where

$$a=\frac{E_{th}e^2}{\varepsilon_0 cm\omega^2 SU_i}-\frac{2m\langle\varepsilon\rangle\tau}{MU_i},$$

$$b=1/\beta\ln(n_b/n_0),$$

$$c=\frac{2\langle\varepsilon\rangle\tau}{3m\Delta^2\beta^2}.$$

A crude estimation performed in our previous work revealed that the term c/a is much smaller than $b/2a$ [37]. Thus, neglecting this term, one notices that the pressure threshold for the breakdown should be directly proportional to the ionization potential of an absorbing gas. To check this hypothesis the P_{th} values were plotted against appropriate U_i values in Fig. 1, where points represent the experimental data and the solid lines are calculated on the basis of the least squares method. As may be noticed the agreement is rather poor. There are at least two reasons which can account for the observed discrepancies. Firstly, the applied theory is, undoubtedly, oversimplified as it does not consider all the parameters influencing the breakdown phenomenon, i.e., some other individual properties of molecules (e.g., polarizabilities), experimental setup, and so on. Secondly, the proportionality coefficient (p), in the relationship: $P_{th}=pU_i$, depends on the individual properties of a given gas. Taking into account the above facts only a qualitative agreement can be expected between theory and experiment. Indeed, the solid lines in Fig. 1 show actually only the qualitative tendency of P_{th} as a function of the ionization potential of an irradiated system. It may perhaps be worthwhile to mention that the relationship given by (3) predicts also a decrease of the pressure threshold for the gas breakdown with a shortening of a laser pulse duration, this dependency being actually observed experimentally (Fig. 1).

2.2. *The Behavior of* H_2–D_2 *System in a Focused* CO_2*-Laser Photon Field*

The interaction of a focused CO_2-laser beam with H_2–D_2 system at a total pressure exceeding the breakdown threshold causes depletion of both parent reactants and formation of HD. The yields of HD formation versus composition of irradiated H_2–D_2 mixture are shown in Fig. 2. The position of the experimental data points is characteristic of reactions proceeding in two component systems when composition changes cover the whole range of possible concentrations [30, 37, 47]. The first impression after reviewing these data is that an equilibrium is attained in the reaction volume. To verify this hypothesis we derived an expression relating the reaction yield

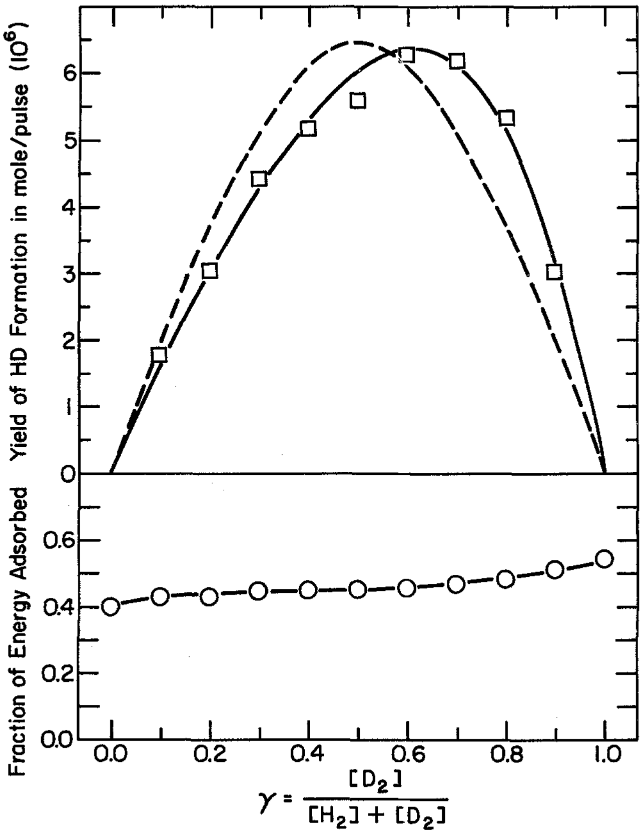

Fig. 2. Fraction of energy absorbed (lower graph) and yield of HD formation (upper graph) versus mole fraction of D_2 upon irradiation of H_2–D_2 mixtures at the total pressure of 9.3×10^4 N/m^2. Points in both graphs represent experimental data. Dashed line in the upper graph corresponds to equilibrium yields of reaction and solid line to the kinetic model prediction. Solid line in the lower graph represents empirical fit to the data with the equation:

$$E_{abs}/E_0 = 0.4(1-\gamma)^{1.6} + 0.54\gamma^{0.76}$$

($Y(\mathrm{HD})_e$) to the initial number of molecules of both parent reactants in the reaction volume ($N_{H_2}+N_{D_2}$), the equilibrium constant (K), and the composition of the reactant mixture (γ), starting from the equation for the equilibrium constant, viz.

$$Y(\mathrm{HD})_e = (N_{H_2}+N_{D_2})\frac{K-\sqrt{K^2-4K(K-1)\gamma(1-\gamma)}}{2(K-1)}. \tag{4}$$

To make any use of (4) one has to know the value of K and the initial amounts of both reactants in the reaction volume. Unfortunately, none of these quantities is known unambiguously. The equilibrium constant varies with temperature according to the equation [32]

$$K = 4.24\exp(-78.8/T). \tag{5}$$

Using (5) we calculated values of the term in (4) that is dependent on K, and we noticed that they change insignificantly with temperature. For example, at $\gamma = 0.5$, where the changes are the most pronounced, we obtained values equal to 0.3218, 0.3278, 0.3322, and 0.3344, corresponding to temperatures [K] equal to 300, 500, 1000, and 2000, respectively. The actual temperature for the process occurring in our system is not known. To proceed further into this problem, however, we assumed the K value corresponding to 298 K. The reaction volume can be expected to be constant, as the total pressure and the experimental setup have been always the same. Unfortunately, though, it can not be predicted with any degree of certainty. Therefore, the expression given by (4) can be used only for fitting the experimental data shown in Fig. 2. The $Y(\mathrm{HD})_e$ values were thus calculated varying $N_{H_2}+N_{D_2}$ in such a way as to obtain the lowest value of the function: $\sum_{\gamma=0.1}^{\gamma=0.9}[Y_\gamma(\mathrm{HD})_{e,\mathrm{cal}} - Y_\gamma(\mathrm{HD})_{\mathrm{exp}}]^2$. This procedure leads to $N_{H_2}+N_{D_2}$ equal to 2.0×10^{-5} mole, which corresponds to a reaction volume of 5.3 cm^3. The calculated equilibrium yields of HD formation are shown as a dotted line in Fig. 2. The derived curve is symmetrical around the $\gamma = 0.5$ axis and its shape is not affected by the temperature. The increase of the latter parameter would cause only minor shifts of $Y(\mathrm{HD})_e$ toward higher values. All the above considerations demonstrate that the system studied apparently does not reach an equilibrium in our experimental conditions. Moreover, this information implies that kinetic phenomena must be responsible for the asymmetrical shape of the reaction yield curve.

Assuming that the major part of the laser-field energy is absorbed via the inverse bremsstrahlung mechanism, one can expect the primary reactive species to be free electrons. Secondary reactive species could be created upon the impact of energized electrons on neutral molecules and these would be positive [33, 48–52] or negative [53] molecular ions, atoms [33, 36, 50, 52, 54–56] and ionized atoms [32, 50, 52, 55]. All the species, including parent molecules of both reactants, can be electronically, vibrationally, rotationally or translationally excited if a given form of excitation is accessible to the molecule [54–56]. These excited species can be formed either upon electron impact dissociation of parent molecules or as a result of inelastic collisions of electrons with any species present in the system. Another possible pathway for creation of reactive states would be via a direct or collisional interaction of the intense ir photon field with some species which could be present in the system studied, e.g., H_2^+, H ... H_2, H^+ ... H_2, etc. Although the latter mechanism of energy absorption can be predicted on the basis of recently reported theoretical considerations [20, 21, 23, 25, 57], and some experimental observations [58], it does not seem to be a major one by which the system absorbs energy from the focused CO_2-laser beam.

To simplify the problem let us consider the following processes to be a consequence of the interaction of an intense CO_2-laser photon field with the system studied (H: hydrogen isotopes):

$$\begin{aligned} H_2 \xrightarrow{\text{laser field}} \; & H_2^+ + e^- , && (6) \\ & H^+ + H + e^- , && (7) \\ & 2H , && (8) \\ & H^+ + H^- . && (9) \end{aligned}$$

The electron impact [52] and proton impact (cosmic radiation) [59] studies reveal that dissociation according to (9) is of very low probability. Similarly, electron attachment processes leading to the creation of negative molecular ions can be neglected [53]. The dissociation channel represented by (7) does not play a major role in the formation of primary reactive species. According to photoionization [60], electron impact [48, 49], and proton impact [59] investigations, the ratio of $[H^+]/[H_2^+]$ is usually lower than 10% and does not depend notably on the amount of energy carried by interacting particles or electromagnetic radiation. Nevertheless, species formed by (7) may contribute to further reaction owing to their high reactivity.

Secondary processes in which the species formed via (6–9) participate, can be categorized by the following groups [61]: ion-molecule reactions, charge neutralization, atom-molecule reactions, and atom recombination. The overall mechanism may, thus, be expected to be very complicated. In order to attempt to rationalize this subject, let us consider the rates of the secondary processes and subsequently the lifetimes of these transients with respect to the particular reaction pathways. This information is compiled in Table 1. All reactions in Table 1 are numbered from (10) to (21) and we will refer to these numbers subsequently in the text.

In order to evaluate lifetimes of intermediate species towards various reaction pathways some assumptions regarding initial concentrations of reactants are necessary. If the entire energy absorbed (ca. 0.72 J/pulse; lower half of Fig. 2) would be used only for the ionization of parent molecules one would expect the formation of 4.8×10^{-7} mole of molecular ions and electrons per pulse via reaction (6) (the mean value of ΔH_{f0}^{0} for H_2^+ and D_2^+ is equal ca. 1490 kJ/mole [71]). One may conclude that virtually each molecule in the focal volume is ionized during the pulse, so initial concentrations of both H_2^+ and e^- would be the same as that of the parent molecules, i.e. 3.75×10^{-6} mole/cm³ (70 Torr). To enable a comparison of probabilities for various processes we assume the concentration of H_3^+ attains ultimately the

Table 1. Reaction scheme

Reaction No.	Process[a]		Rate constant[b]	Half-lifetime [s]	Ref.
(10)	$H_2^+ + e^-$	$\rightarrow 2H$	5.9×10^{15}	4.5×10^{-11}	[62]
(11)	$H_2^+ + H_2$	$\rightarrow H_3^+ + H$	1.3×10^{15}	1.4×10^{-10}	[59]
(12)	$H^+ + e^-$	$\rightarrow H + h\nu$	2.1×10^{12}	9.1×10^{-8}	[59]
(13a)	$H^+ + D_2$	$\rightarrow HD + D^+$	2.2×10^{14}	8.4×10^{-10}	[32]
(13b)	$D^+ + H_2$	$\rightarrow HD + H^+$	1.0×10^{15}	1.8×10^{-10}	[32]
(14)	$H^+ + H_2$	$\rightarrow H_3^+ + h\nu$	$\sim 6 \times 10^{4}$	3.1	[63]
(15)	$H^+ + H_2$	$\rightarrow H_3^+$		$< 5 \times 10^{-11}$	[64]
(16)	$H^+ + H_2 + H_2$	$\rightarrow H_3^+ + H_2$	1.2×10^{19}	4.1×10^{-9}	[65]
(17)	$H_3^+ + e^-$	$\rightarrow H_2(2H) + H$	1.1×10^{16}	2.4×10^{-11}	[66]
(18)	$H_3^+ + HD$	$\rightarrow H_2 + H_2D^+$	6.6×10^{14}	2.8×10^{-10}	[67]
(19a)	$H + D_2$	$\rightarrow HD + D$	1.1×10^{7}	1.7×10^{-2}	[31]
(19b)	$D + H_2$	$\rightarrow HD + H$	1.3×10^{8}	1.4×10^{-3}	[31]
(20a)	$H + H + M$	$\rightarrow H_2 + M$	3.3×10^{15}	5.4×10^{-6}	[68]
(20b)	$H + D + M$	$\rightarrow HD + M$			
(20c)	$D + D + M$	$\rightarrow D_2 + M$	4.0×10^{15}	4.4×10^{-6}	[69][c]
(21a)	H	$\xrightarrow{\text{wall}} 1/2\,H_2$	4.2	1.7×10^{-1}	[70][d]
(21b)	D	$\xrightarrow{\text{wall}} 1/2\,D_2$	3.3	2.1×10^{-1}	[70][d]

[a] Symbol M denotes bath molecules

[b] All values correspond to the ambient temperature. Units: 1/s, cm³/(mole s), and cm⁶/(mole² s) for the first, second, and third order reactions, respectively

[c] Value calculated from the dependency: $k(T) = 1.2 \times 10^{18}\, T^{-1}$ (see text)

[d] For information see text

same value as that of H_2^+, whereas, concentrations of H and D are twice those corresponding to the originally produced ionic species. Lastly, the concentrations of H^+ and D^+ were assumed to be 1/10 of that for H_2^+ on the basis of previous considerations.

The above assumed values do not reflect real concentrations of reaction transients; nevertheless, they facilitate the drawing of some qualitative conclusions. The main reaction transients, i.e. positive molecular ions, disappear via the very fast process (10) or alternatively by reactions (11) and (17). Process (18), which could contribute to the hydrogen-deuterium exchange, can not compete with (17) owing to the relatively low rate and deficiency of parent molecules in the focal zone. For atomic ions several pathways are available. Some of these species may disappear via radiative association (12) and this process seems to be one which can account for the visible luminescence that always accompanied the absorption of energy from the laser beam. Reaction (14) is too slow to play any role in the decay of atomic ions. Both bimolecular (15) and trimolecular (16) channels followed by a very fast process (17) are the main pathways for the concumption of these species. The only processes which could compete with them would be reactions (13a) and (13b) and both processes can contribute to the formation of HD. Taking into account, however, that initial aboundances of atomic ions are much lower than these of molecular ions and that charge neutralization processes are very fast, one can expect this contribution to be minor.

Some further consequences arise from the above considerations. Owing to the high density of positive ions and electrons in the focal volume and attractive interactions between them, the neutralization processes are so fast that any other processes involving ions can not compete. Combining this information with the fact that some transients are also created via (8), one comes to the conclusion that only atomic species are directly significant in causing the H_2–D_2 exchange reaction.

The time in which primary intermediates are created [reactions (6–9)] is not known exactly, however, it should be shorter than the pulse duration ($\sim 10^{-7}$ s) [56]. Since lifetimes for the decay of all ionic species are much shorter one may assume for chemical kinetic consideration that H and D atoms are instantaneously created by the ir laser photon field in the focal zone.

The experimental yields of HD formation are several times higher than the amounts of atoms estimated earlier to be originally produced by the pulse. Thus, chain reactions must play an important role in HD formation. The crude estimations of the lifetimes of atomic transients with respect to the various reaction pathways (Table 1) reveal that atom-atom combination processes can compete with chain propagation steps [reaction (19a and 19b)] early in the pulse. On the other hand, the relatively slow diffusion processes of atoms to the walls are the only alternatives for termination steps (20a–c) and they must play a predominant role at the end of the process when atomic concentrations are low and the probabilities for encounter of two atoms become very low.

The concentrations of the reaction transients change significantly with time and, therefore, the application of the steady-state approximation to the examination of kinetics does not seem to be adequate. The amounts of H and D do not change in the chain propagation steps but rather only in the depletion processes (20a–21b). Thus, the rate equations for the decay of these species, according to the mechanism (Table 1), are

$$-\frac{d[\mathrm{H}]}{dt}=2k_{20\mathrm{a}}[\mathrm{H}]^2[\mathrm{M}] + k_{20\mathrm{b}}[\mathrm{H}][\mathrm{D}][\mathrm{M}]+k_{21\mathrm{a}}[\mathrm{H}]\,, \tag{22}$$

$$-\frac{d[\mathrm{D}]}{dt}=2k_{20\mathrm{c}}[\mathrm{D}]^2[\mathrm{M}] + k_{20\mathrm{b}}[\mathrm{H}][\mathrm{D}][\mathrm{M}]+k_{21\mathrm{b}}[\mathrm{D}]\,. \tag{23}$$

Since the amount of energy absorbed does not change markedly with γ we assume that the sum of initial concentrations of $\mathrm{H}([\mathrm{H}]_0)$ and $\mathrm{D}([\mathrm{D}]_0)$ is independent of composition and that the initial concentrations of individual species are proportional to the amounts of their precursors in the mixture, i.e. $[\mathrm{H}]_0=(1-\gamma)([\mathrm{H}]_0+[\mathrm{D}]_0)$ and $[\mathrm{D}]_0=\gamma([\mathrm{H}]_0+[\mathrm{D}]_0)$. The functional dependence relating [H] and [D] is not known. To make the problem tractable we assume that the relative concentrations of intermediate species do not change during the course of the process, i.e. $[\mathrm{H}]=(1-\gamma)([\mathrm{H}]+[\mathrm{D}])$ and $[\mathrm{D}]=\gamma([\mathrm{H}]+[\mathrm{D}])$. Substituting appropriate relationships resulting from the above dependencies into (22 and 23) and integrating, one obtains expressions for the concentrations of the reaction transients as a function of time (t) after formation by the pulse, viz.

$$[\mathrm{H}]=\frac{(1-\gamma)k_{21\mathrm{a}}([\mathrm{H}]_0+[\mathrm{D}]_0)\exp(-k_{21\mathrm{a}}t)}{[2(1-\gamma)k_{20\mathrm{a}}[\mathrm{M}]+\gamma k_{20\mathrm{b}}[\mathrm{M}]]([\mathrm{H}]_0+[\mathrm{D}]_0)(1-[1-\exp(-k_{21\mathrm{a}}t)])+k_{21\mathrm{a}}}, \tag{24}$$

$$[\mathrm{D}]=\frac{\gamma k_{21\mathrm{b}}([\mathrm{H}]_0+[\mathrm{D}]_0)\exp(-k_{21\mathrm{b}}t)}{[2\gamma k_{20\mathrm{c}}[\mathrm{M}]+(1-\gamma)k_{20\mathrm{b}}[\mathrm{M}]]([\mathrm{H}]_0+[\mathrm{D}]_0)(1-[1-\exp(-k_{21\mathrm{b}}t)])+k_{21\mathrm{b}}}. \tag{25}$$

Following the reaction scheme the rate of HD formation is given by (26):

$$\frac{d[\mathrm{HD}]}{dt}=k_{19a}[\mathrm{H}]\,[\mathrm{D}_2]+k_{19b}[\mathrm{D}]\,[\mathrm{H}_2]+k_{20b}[\mathrm{H}]\,[\mathrm{D}]\,[\mathrm{M}]\,. \tag{26}$$

The term resulting from the process (20b) can be neglected owing to its minor contribution to the HD formation. If we now substitute (24 and 25) into (26) and integrate, we may obtain an equation for the yield of HD formation, $Y(\mathrm{HD})$, by evaluation of the resulting expression as $t\rightarrow\infty$, viz.

$$\begin{aligned}Y(\mathrm{HD})=(N^0_{\mathrm{H}_2}+N^0_{\mathrm{D}_2})&\left\{\frac{\gamma(1-\gamma)k_{19a}}{2(1-\gamma)k_{20a}[\mathrm{M}]+\gamma k_{20b}[\mathrm{M}]}\ln\left[1+[2(1-\gamma)k_{20a}[\mathrm{M}]+\gamma k_{20b}[\mathrm{M}]]\cdot\frac{[\mathrm{H}]_0+[\mathrm{D}]_0}{k_{21a}}\right]\right.\\&\left.+\frac{\gamma(1-\gamma)k_{19b}}{2\gamma k_{20c}[\mathrm{M}]+(1-\gamma)k_{20b}[\mathrm{M}]}\cdot\ln\left[1+[2\gamma k_{20c}[\mathrm{M}]+(1-\gamma)k_{20b}[\mathrm{M}]]\frac{[\mathrm{H}]_0+[\mathrm{D}]_0}{k_{21b}}\right]\right\},\end{aligned} \tag{27}$$

where $N^0_{\mathrm{H}_2}+N^0_{\mathrm{D}_2}$ denotes the initial number of moles of H_2 and D_2 in the reaction cell.

The expression given by (27) is not amenable to testing by plotting of some simple function of $Y(\mathrm{HD})$ against γ. Therefore, let us consider features of this dependency under boundary conditions. As one may expect, $Y(\mathrm{HD})$ becomes equal to 0 if γ reaches 0 or 1. The differentiation of $Y(\mathrm{HD})$ with respect to γ leads to a rather cumbersome equation which admits, however, quite simple forms in boundary conditions, i.e. (28 and 29), viz.

$$\begin{aligned}\lim_{\gamma\rightarrow 0}\frac{dY(\mathrm{HD})}{d\gamma}&=(N^0_{\mathrm{H}_2}+N^0_{\mathrm{D}_2})\\&\cdot\left[\frac{k_{19a}}{2k_{20a}[\mathrm{M}]}\ln\left(1+2k_{20a}[\mathrm{M}]\frac{[\mathrm{H}]_0+[\mathrm{D}]_0}{k_{21a}}\right)+\frac{k_{19b}}{k_{20b}[\mathrm{M}]}\ln\left(1+k_{20b}[\mathrm{M}]\frac{[\mathrm{H}]_0+[\mathrm{D}]_0}{k_{21b}}\right)\right],\end{aligned} \tag{28}$$

$$\begin{aligned}\lim_{\gamma\rightarrow 1}\frac{dY(\mathrm{HD})}{d\gamma}&=-(N^0_{\mathrm{H}_2}+N^0_{\mathrm{D}_2})\\&\cdot\left[\frac{k_{19b}}{2k_{20c}[\mathrm{M}]}\ln\left(1+2k_{20c}[\mathrm{M}]\frac{[\mathrm{H}]_0+[\mathrm{D}]_0}{k_{21b}}\right)+\frac{k_{19a}}{k_{20b}[\mathrm{M}]}\ln\left(1+k_{20b}[\mathrm{M}]\frac{[\mathrm{H}]_0+[\mathrm{D}]_0}{k_{21a}}\right)\right].\end{aligned} \tag{29}$$

All rate coefficients in the above relationships depend significantly on temperature which, unfortunately, can not be predicted with any degree of certainty. Also, the initial concentration of reaction transients is impossible to estimate directly. Therefore, (27) can be used only as an approximate formula to fit the experimental data shown in Fig. 2. For this purpose the knowledge of the temperature dependencies of all rate constants is required. Expressions for $k_{19a}(T)$ and $k_{19b}(T)$, derived on the basis of the work Garrett and Truhlar [31] who calculated rate coefficients in the region 200–4000 K, are taken to be

$$\left.\begin{aligned}k_{19a}(T)&=1.63\times10^{15}\exp(-952.8/T^{0.69})\\k_{19b}(T)&=2.13\times10^{15}\exp(-593.2/T^{0.63})\end{aligned}\right\}\ \text{in cm}^3/\text{(mole s)}.$$

The above equations correspond to the values for the CVT/MCPVAG model which best correlates with the experimental data. The $k_{20a}(T)$ functional dependence was taken directly from [68], whereas, $k_{20c}(T)$ has been established on the basis of the experimental data reviewed in [69]

$$\left.\begin{aligned}k_{20a}(T)&=1.0\times10^{17}\,T^{-0.6}\\k_{20c}(T)&=1.2\times10^{18}\,T^{-1}\end{aligned}\right\}\ \begin{aligned}&\text{in cm}^6/(\text{mole}^2\ \text{s})\\&(300\text{–}5000\ \text{K}).\end{aligned}$$

Values of $k_{20b}(T)$, representing the cross-combination rate constant, were evaluated from the expression: $2[k_{20a}(T)+k_{20c}(T)]^{1/2}$ [72]. The crude estimation based on the kinetic theory of gases [73] and available data for the recombination coefficients of hydrogen atoms on metal surfaces [74, 75] suggests that diffusion of the atoms through the gas volume is the rate-controlling step in wall termination. The value of k_{21a} taken from the work of Lynch and Michael [70] is equal to 4.2 s^{-1} at ambient temperature. The corresponding rate constant for the diffusion of D atoms was estimated from k_{21a}, assuming that the only difference between the diffusion rates of H and D atoms results from their masses. This leads to a value for k_{21b} of 3.3 s^{-1}. Study of the temperature dependence of the diffusion coefficient of H atoms in H_2 indicates that $D\sim T^{3/2}$ [76] and, combining these facts, one may write

$$k_{21a}=4.2(T/300)^{3/2}\ [\mathrm{s}^{-1}],$$

$$k_{21b}=3.3(T/300)^{3/2}\ [\mathrm{s}^{-1}].$$

Substituting now the appropriate $k(T)$ dependencies into (27) and taking $N^0_{\mathrm{H}_2}+N^0_{\mathrm{D}_2}=5.7\times10^{-4}$ mole and $[\mathrm{M}]=3.75\times10^{-6}$ mole/cm^3, we varied $[\mathrm{H}]_0+[\mathrm{D}]_0$ and T in such a way as to obtain the best fit to the experimental values. In the first approximation we assumed constant temperature for the process. Since $k_{19b} > k_{19a}$ the second term of the right-hand side of (27) always contributes more to the Y(HD) than the first one. This implies that the asymmetry of the reaction yield curve, predicted with the above assumption, is such that the maximum occurs on the low side of $\gamma = 0.5$ axis. It is worth noting that a similar dependency can be expected in the case of an ionic mechanism, since kinetic isotope effects for these processes would be in the same direction (Table 1). To find an explanation for the asymmetry of the experimental Y(HD) curve we assume that the temperature of the process changes with the composition of the reactant mixture. Actually one might expect such a phenomenon by examining the absorption curve seen in the lower half of Fig. 2. Assuming that the entire energy absorbed would be used for heating the gas sample, one would expect an increase of the macroscopic temperature of the system by 39 K in the case of pure H_2 and ca. 52 K for D_2. This difference is presumably higher around the focal zone. Assuming thus that temperature of the system varies linearly with γ, we obtained the fit shown as a solid line in Fig. 2 if $[H]_0 + [D]_0 = 3.6 \times 10^{-10}$ mole/cm^3 and $T = 335 + 35\gamma$ [K].

The purely phenomenological approach to the problem presented in this work allows one to draw some further conclusions. Substitution of appropriate values of the derived parameters into the expressions for the limiting slopes obtained under the boundary conditions, leads to the values of 1.6×10^{-5} and 3.7×10^{-5} mole/pulse for $\gamma = 0$ and 1, respectively. Both (28 and 29) are two-term expressions. The first term of (28) and the second term of (29) represent contributions to the Y(HD) from the reactions initiated by H atoms ($Y(\mathrm{HD})_\mathrm{H}$), whereas, the remaining two terms of both these equations correspond to processes initiated by D atoms ($Y(\mathrm{HD})_\mathrm{D}$). The ratios of $Y(\mathrm{HD})_\mathrm{D}/Y(\mathrm{HD})_\mathrm{H}$, estimated on the basis of parameters derived earlier, are equal to 11.1 as $\gamma \to 0$ and 9.1 when $\gamma \to 1$. These ratios describe the kinetic isotope effect in the CO_2 laser-induced exchange in the H_2–D_2 system. It is worth mentioning that the ratios derived above are in satisfactory agreement with the ratios of rate constants for the atom molecule reaction [31], a fact tending to confirm the radical nature of secondary processes.

Since much larger amounts of atoms than estimated from the kinetic model may be expected to be produced by the pulse, there must exist some pathways for fast consumption of these species. It is likely that they disappear in termolecular combination processes. These processes should be favored owing to the high density of atoms in the focal region.

The chain length can be defined as the number of HD molecules formed per atom produced by the pulse. If we assume that the sum of $[H]_0$ and $[D]_0$ is related to the whole reaction cell then 5.5×10^{-8} mole of atoms initiate chain processes. Combining this estimation with the reaction yield at $\gamma = 0.5$ leads to a value for the chain length of ca. 110. Although this value can be considered only as a rough estimate, nevertheless, it is consistent with the assumption of the radical nature of the secondary processes [77].

The question remains of how to explain the differences in the energy absorption by H_2 and D_2 molecules. We have mentioned earlier in the text that some theoretical considerations predict the possibility of direct ir energy absorption by some species which can be present in the system studied, e.g. $H \ldots H_2, H_3^+$, and so on. If this mechanism truly exists, the probability for energy absorption would be higher in the case of deuterium species owing to the higher density of their vibrational states. The same feature of D_2 molecules causes the increased vibrational heat capacity and thus the accumulation of energy increases with increasing amounts of D_2 in the system.

Acknowledgements. This work was supported by Contract No. DE-AS02-76ER03416 with the U.S. Department of Energy.

References

1. N.A. Generalov, V.P. Zimanov, G.I. Kozlov, V.A. Masyukov, Yu.P. Raizer: Pis'ma Zh. Eksp. Teor. Fiz. **11**, 343 (1970)
2. D.C. Smith: J. Appl. Phys. **41**, 4501 (1970)
3. D.C. Smith: Appl. Phys. Lett. **19**, 405 (1971)
4. G.A. Hill, D.J. James, S.A. Ramsden: J. Phys. D. **5**, L97 (1972)
5. A.A. Offenberger, N.H. Brunett: J. Appl. Phys. **43**, 4977 (1972)
6. N.G. Basov, E.M. Belenov, V.A. Danilychev, O.M. Kerimov, I.B. Kovsh: Zh. Eksp. Teor. Fiz. **63**, 2010 (1972)
7. R.T. Brown, D.C. Smith: Appl. Phys. Lett. **22**, 245 (1973)
8. M.P. Hacker, D.R. Cohn, B. Lax: Appl. Phys. Lett. **23**, 392 (1973)
9. C.H. Chan, C.D. Moody, W.B. McKnight: J. Appl. Phys. **44**, 1179 (1973)
10. C.D. Moody: Appl. Phys. Lett. **22**, 31 (1973)
11. M.P. Hacker, D.R. Cohn, R.L. Brooks: Appl. Phys. Lett. **24**, 173 (1974)
12. N.H. Burnett, A.A. Offenberger: J. Appl. Phys. **45**, 623 (1974)
13. P. Behrens: U.S.N.T.I.S., AD Rep. 1974, No. 783855/OGA; C.A. **82**, 131784z (1975)
14. D.R. Cohn, M.P. Hacker, B. Lax, W. Halverson: J. Appl. Phys. **46**, 668 (1975)
15. C.G. Morgan: Rep. Prog. Phys. **38**, 621 (1975)
16. G.I. Kozlov: Zh. Tekh. Fiz. **49**, 67 (1979)
17. G. Roy, Y. D'Astous, M. Blanchard, R. Tremblay: Can. J. Phys. **58**, 1477 (1980)
18. P.E. Nielsen, G.H. Canavan: J. Appl. Phys. **44**, 4224 (1973)
19. C.H. Chan, C.D. Moody: J. Appl. Phys. **45**, 1105 (1974)

20. P. Fournier, B. Lassier-Govers, G. Comtet: Springer Ser. Chem. Phys. 6 (Laser-Induced Processes Mol.), 247 (1979)
21. A.E. Orel, W.H. Miller: J. Chem. Phys. **72**, 5139 (1980)
22. G.V. Gomelauri, A.S. Epifanov, A.A. Manenkov, A.M. Prokhorov: Zh. Eksp. Teor. Fiz. **79**, 2356 (1980)
23. M. Mohan: J. Chem. Phys. **75**, 1772 (1981)
24. R.T. Bailey, F.R. Cruickshank, D. Pugh, W. Johnstone: J. Chem. Soc., Faraday Trans. II **77**, 1387 (1981)
25. M. Mohan: Mol. Phys. **50**, 1251 (1983)
26. F.F. Kormendi: Opt. Acta **31**, 301 (1984)
27. D.G. Truhlar, R.E. Wyatt: Ann. Rev. Phys. Chem. **27**, 1 (1976)
28. L.L. Lohr: Chem. Phys. Lett. **56**, 28 (1978)
29. M. Kneba, U. Wellhausen, J. Wolfrum: Ber. Bunsenges. Phys. Chem. **83**, 940 (1979)
30. S.H. Bauer: Ann. Rev. Phys. Chem. **30**, 271 (1979)
31. B.C. Garrett, D.G. Truhlar: J. Chem. Phys. **72**, 3460 (1980)
32. M.J. Henchman, N.G. Adams, D. Smith: J. Chem. Phys. **75**, 1201 (1981)
33. S.L. Anderson, F.A. Houle, D. Gerlich, Y.T. Lee: J. Chem. Phys. **75**, 2153 (1981)
34. J.M. Bowman, K.-T. Lee, R.B. Walker: J. Chem. Phys. **79**, 3742 (1983)
35. A. Lifshitz, M. Badini, H.F. Carroll: J. Chem. Phys. **79**, 2742 (1983)
36. H. Tsuruta, T. Mlyazaki, K. Fueki, N. Azuma: J. Phys. Chem. **87**, 5422 (1983)
37. J. Blazejowski, F.W. Lampe: J. Appl. Phys. **59**, 2283 (1986)
38. K.W. Saunders, H.A. Taylor: J. Chem. Phys. **9**, 616 (1941)
39. A. Schwebel, A.M. Ronn: J. Phys. Chem. **87**, 4375 (1983)
40. J.D. Campbell, G. Hancock, J.B. Halpern, K.H. Welge: Chem. Phys. Lett. **44**, 404 (1976)
41. Y. Ishikawa, O. Kurihara, R. Nakane, S. Arai: Chem. Phys. **52**, 143 (1980)
42. V.E. Merchant: Opt. Commun. **25**, 259 (1978)
43. S.V. Filseth, J. Danon, D. Feldmann, J.D. Campbell, K.H. Welge: Chem. Phys. Lett. **63**, 615 (1979)
44. P. Avouris, I.Y. Chan, M.M.T. Loy: J. Chem. Phys. **72**, 3522 (1980)
45. Y. Langsam, A.M. Ronn: Chem. Phys. **54**, 277 (1981)
46. A.M. Ronn: Chem. Phys. Lett. **42**, 202 (1976)
47. S.H. Bauer, D.M. Lederman, E.L. Resler, E.R. Fischer: Int. J. Chem. Kinet. **5**, 93 (1973)
48. D. Rapp, P. Englander-Golden, D.D. Briglia: J. Chem. Phys. **42**, 4081 (1965)
49. C. Backx, G.R. Wight, M.J. Van der Wiel: J. Phys. B **9**, 315 (1976)
50. K. Koellmann: J. Phys. B **11**, 339 (1978)
51. M.D. Burrows, L.C. McIntyre, S.R. Ryan, W.E. Lamb: Phys. Rev. A **21**, 1841 (1980)
52. M. Landau, R.I. Hall, F. Pichou: J. Phys. B **14**, 1509 (1981)
53. R. Schnitzer, R.W. Odom, M. Anbar: J. Chem. Phys. **68**, 1489 (1978)
54. M. Capitelli, M. Dilonardo: Chem. Phys. **20**, 417 (1977)
55. T. Ogawa, M. Higo: Chem. Phys. **52**, 55 (1980)
56. M. Capitelli, E. Molinari: Top. Curr. Chem. **90**, 59 (1980)
57. S.-I. Chu, C. Laughlin, K.K. Dutta: Chem. Phys. Lett. **98**, 476 (1983)
58. A. Carrington, J. Buttenshaw: Mol. Phys. **44**, 267 (1981)
59. S.S. Prasad, W.T. Huntress: Astrophys. J. Suppl. **43**, 1 (1980)
60. T. Masuoka: J. Chem. Phys. **81**, 2652 (1984)
61. D. Smith, N.G. Adams: Pure Appl. Chem. **56**, 175 (1984)
62. A. Giusti-Suzor, J.N. Bardsley, C. Derkits: Phys. Rev. A **28**, 682 (1983)
63. W.T. Huntress: In *Interactions between Ions and Molecules*, ed. by P. Ausloos. Nato Advanced Study Institutes Series, Ser. B: Physics (Plenum, New York 1975) p. 642
64. Ch. Schlier, W. Vix: Chem. Phys. **95**, 401 (1985)
65. R. Johnsen, M.A. Biondi: J. Chem. Phys. **61**, 2112 (1974)
66. N.G. Adams, D. Smith, E. Alge: J. Chem. Phys. **81**, 1778 (1984)
67. N.G. Adams, D. Smith: Astrophys. J. **248**, 373 (1981)
68. N. Cohen, K.R. Westberg: J. Phys. Chem. Ref. Data **12**, 531 (1983)
69. D.L. Baulch, D.D. Drysdale, D.G. Horne, A.C. Lloyd: *Evaluated Kinetic Data for High Temperature Reactions*, Vol. 1 (CRS Press, Cleveland, OH 1972) p. 289
70. K.P. Lynch, J.V. Michael: Int. J. Chem. Kinet. **10**, 233 (1978)
71. H.M. Rosenstock, K. Draxl, B.W. Steiner, J.T. Herron: J. Phys. Chem. Ref. Data **6**, Suppl. 1 (1977)
72. A. Lifshitz, M. Frenklach: J. Chem. Phys. **67**, 2803 (1977)
73. S.W. Benson: *The Foundation of Chemical Kinetics* (McGraw-Hill, New York 1960) p. 446
74. M.U. Kislyuk, I.I. Tret'yakov: Dokl. Akad. Nauk. SSSR **208**, 1134 (1973)
75. M.U. Kislyuk, I.I. Tret'yakov: Kinet. Katal. **15**, 710 (1974)
76. K.M. Sancier, H. Wise: J. Chem. Phys. **51**, 1434 (1969)
77. S.O. Thompson, O.A. Schaeffer: J. Am. Chem. Soc. **80**, 553 (1958)